

# The Nucleon-Nucleon Interaction and Large $N_c$ QCD

Manoj K. Banerjee, Thomas D. Cohen and Boris A. Gelman  
*Department of Physics, University of Maryland, College Park, MD 20742-4111.*

The nature of the nonrelativistic nucleon-nucleon potential in the large  $N_c$  limit is discussed. In particular, we address the consistency of the meson exchange picture of nucleon interactions. It is shown that the nonrelativistic nucleon-nucleon potential extracted from the Feynmann graphs up to and including two-meson exchange diagrams satisfies the spin-flavor counting rules of Kaplan and Savage, and Kaplan and Manohar, provided the nucleon momenta is of order  $N_c^0$ . The key to this is a cancelation of the retardation effect of the box graphs against the contributions of the crossed-box diagram. The consistency requires including  $\Delta$  as an intermediate state.

## I. INTRODUCTION

One of the most fundamental problems in nuclear physics is to understand how low-energy nucleon-nucleon interactions arise from the underlying quark-gluon interactions. Unfortunately, for some time to come QCD is likely to remain computationally intractable in this regime in the sense that one will not be able to directly predict the values of low energy nuclear physics observables by calculations based solely on the QCD Lagrangian. Nevertheless one might hope to be able to deduce some qualitative (or perhaps semi-quantitative) features of nucleon-nucleon interactions from our knowledge of QCD. The known simplifications of certain aspects of QCD in the large  $N_c$  limit could provide such a tool [1-5]. Indeed, several years ago it was proposed that the spin-flavor structure of the dominant terms in the nucleon-nucleon potential can be understood in terms of large  $N_c$  QCD [6,7]. As we shall argue here large  $N_c$  QCD can provide additional insights into the nature of the nucleon-nucleon force. In particular large  $N_c$  QCD helps us to understand both the nature of the meson-exchange picture of nucleon-nucleon interactions and the limitations of such a picture. The large  $N_c$  perspective also sheds light on the role of the  $\Delta$  resonance in nucleon-nucleon interactions. At a practical level, knowledge of the special role played by  $\Delta$  in canceling certain large contributions may prove to be useful in constructing nucleon-nucleon interactions.

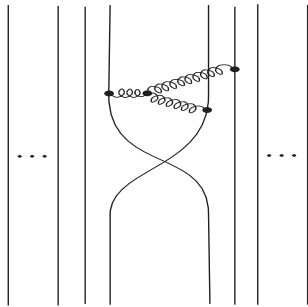


FIG. 1. A typical diagram of order  $N_c$  contributing to the nucleon-nucleon scattering in the large  $N_c$  limit.

The first treatment of nucleon-nucleon interactions in large  $N_c$  QCD was done by Witten in his seminal paper on baryons in the large  $N_c$  limit [2]. He argued that the dominant interaction between two baryons is generically of order  $N_c$ . His argument was based on consideration of diagrams such as the one in Fig. 1. It is clear that such a diagram is order  $N_c$ —a factor  $N_c^3$  from combinatorics and a factor of  $N_c^{-2}$  from the coupling constants. It is straightforward to see that all quark-line-connected graphs beginning and ending with two flavor singlet combinations of  $N_c$  quarks will be  $\mathcal{O}(N_c)$  or less. However, this interaction strength of order  $N_c$  cannot represent the strength of the nucleon-nucleon scattering amplitude. In the first place, unitarity implies that the scattering amplitude does not grow without a bound as  $N_c$  goes to infinity. Secondly, one can consider graphs like Fig. 2 which although disconnected at the quark level, contribute at the nucleon-nucleon level to the full interaction. It is straightforward to see that the graph in Fig. 2 is order  $N_c^2$  so that the interaction cannot simply go as  $N_c$ . One natural way to interpret the physics contained in the diagrams typified by Figs. 1 and 2 is to argue that they get translated at the hadronic level to contributions from

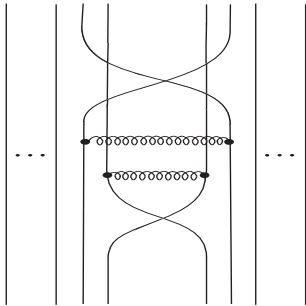


FIG. 2. A typical diagram of order  $N_c^2$ .

nucleon-meson diagrams as in Figs. 3 and 4. In such a hadron-based picture the  $\mathcal{O}(N_c^2)$  contribution then appears as the iteration of an underlying  $\mathcal{O}(N_c)$  interaction. One key issue addressed in this paper concerns the nature of the translation from the quark-gluon based diagrams of Figs. 1 and 2 to the hadronic based ones of Figs. 3 and 4.

Witten [2] noted an additional difficulty of having nucleon-nucleon interaction scaling as  $N_c$ , there is no description of the scattering process which possesses a smooth large  $N_c$  limit if the momenta are of order unity. The basic difficulty in this case is that the kinetic energy of the nucleons is generically much smaller than the potential energy and the interplay of kinetic and potential energy which is at the crux of scattering cannot be independent of  $N_c$ . Witten noted that if one works in a kinematic regime with momenta of order  $N_c$  (*i.e.* an approach to the large  $N_c$  limit with the nucleon velocities rather than momenta fixed), then the kinetic and potential terms are of the same order so that a smooth limit is possible. For this kinematic regime Witten suggested that the scattering process can be described using the time-dependent Hartree (TDH) approximation. It is straightforward to see that the TDH equations with fixed initial velocity have solutions which are independent of  $N_c$ . In practice, such TDH calculations have not been done in QCD and would be very difficult for systems with light quarks.

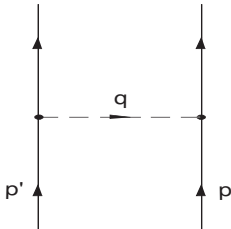


FIG. 3. A one-meson exchange diagram contributing to the nucleon-nucleon potential; initial and final nucleons are on shell;  $p = (|\vec{p}|^2/2m_N, -\vec{p})$ ,  $p' = (|\vec{p}'|^2/2m_N, \vec{p}')$  and  $q = (q^0, \vec{q})$  are energy-momentum 4-vectors flowing through the various lines.

Here we wish to focus on a different limit than Witten's, *i.e.* on low momentum nuclear reactions. Accordingly we do not wish to let the nucleon momenta scale with  $N_c$ ; rather we will restrict our attention to the kinematic regime of nucleon momenta of order  $N_c^0$ . As noted by Witten, in such a regime there is no smooth expression for the scattering amplitude. However, as argued by Kaplan and Savage [6] and Kaplan and Manohar [7] in this regime one may identify the nucleon-nucleon interaction from the quark line connected pieces as a nonrelativistic potential which has a dominant contribution of order  $N_c$ . Such a description can be interpreted on the hadronic level as a meson exchange. The one-meson exchange potential (Fig. 3) can be as large as  $\mathcal{O}(N_c)$  since a generic baryon-meson coupling is of order  $\sqrt{N_c}$  [2] and hence the large  $N_c$  scaling at the hadronic level is consistent with the quark-gluon level. The key insight of Refs. [3–5] is that large  $N_c$  QCD implies an approximate contracted  $SU(4)$  spin-isospin symmetry on the baryons and that this symmetry imposes constraints on the dominant parts of the potential. Thus, the dominant part of the nucleon-nucleon interaction are constrained to be contracted  $SU(4)$  symmetric and terms which break this symmetry are suppressed by two powers of  $N_c$ . For example, the dominant ( $\mathcal{O}(N_c)$ ) contribution to the tensor force is proportional to  $\vec{\tau}_1 \cdot \vec{\tau}_2$ , while the isospin independent part only contributes at order  $N_c^{-1}$ .

This paper will address a number of issues connected with the nucleon-nucleon interaction in large  $N_c$  QCD. One central issue is the identification of the connected diagrams, such as Fig. 3, as a nonrelativistic potential (of order

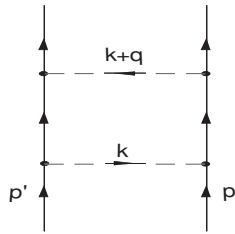


FIG. 4. A box diagram;  $p = (|\vec{p}|^2/2m_N, -\vec{p})$ ,  $p' = (|\vec{p}'|^2/2m_N, \vec{p}')$ ,  $k = (k^0, \vec{k})$  and  $q = (q^0, \vec{q})$  are energy-momentum 4-vectors.

$N_c$ ), as was done in Refs. [6,7]. The argument for doing this is clearly heuristic and is based on the notion that large interactions must be iterated to all orders. Of course, a potential used in a Schrödinger equation is iterated to all orders. This interpretation seems to resolve in a simple manner the order  $N_c^2$  contributions of Fig. 4; it is just one iteration of the potential (among an infinite number of possible iterations).

Unfortunately, this heuristic argument is not unique: an alternative argument would be to identify such an interaction with a kernel of a Bethe-Salpeter equation (with a strength of order  $N_c$ ) which again is to be iterated to all orders. Moreover, it is by no means clear that these are equivalent—a Bethe-Salpeter kernel of order  $N_c$  does not necessarily imply that the potential in a nonrelativistic reduction of the Bethe-Salpeter equation is order  $N_c$ . Thus, at the fundamental level it has to be established whether large  $N_c$  QCD is consistent with a nonrelativistic nucleon-nucleon potential of order  $N_c$  or with a Bethe-Salpeter kernel of order  $N_c$ .

A second fundamental issue in this paper is the extent to which large  $N_c$  QCD justifies a meson exchange picture of nucleon-nucleon interactions. A meson exchange is a natural way to understand nucleon-nucleon interactions as arising from QCD: QCD leads to the existence of colorless hadronic states—baryons and mesons—and the interactions between baryons arise from the exchange of virtual mesons. Indeed, some phenomenologically successful nucleon-nucleon potentials are based directly on a meson exchange picture [8]. On the other hand, the argument for meson exchange dominating the nucleon-nucleon interaction is not compelling and many equally successful nucleon-nucleon potentials include only one-pion exchange treating all shorter distance effects purely phenomenologically [9]. At first sight it might seem that large  $N_c$  arguments do not support the meson-exchange picture of nucleon-nucleon interactions. In the first place, as noted by Witten [2] baryons in the large  $N_c$  behave as solitons, and when two solitons are brought close enough to interact each one distorts in the presence of the other yielding effects which cannot be easily described in terms of meson exchange. Indeed Witten's prescription for scattering for momenta of order  $N_c$ , TDH, necessarily builds in these non-meson-exchange type effects; the clusters of  $N_c$  quarks which interact in TDH are *not* simply the Hartree wave-functions for two nucleons.



FIG. 5. Triangle diagrams;  $p = (|\vec{p}|^2/2m_N, -\vec{p})$ ,  $p' = (|\vec{p}'|^2/2m_N, \vec{p}')$ ,  $k = (k^0, \vec{k})$  and  $q = (q^0, \vec{q})$  are energy-momentum 4-vectors.

There is a second reason why one might suspect that large  $N_c$  QCD does not justify a meson exchange point of view for nucleon-nucleon interactions. The meson-exchange picture does not imply only single meson exchanges but two or more meson exchanges as well. Consider, the large  $N_c$  scaling of a generic two-meson exchange process. Some typical diagrams contributing to the potential are shown in Fig. 5, in which two exchange mesons are coupled to one of the nucleons at a single vertex. Such diagrams are generically of order  $N_c$  since the coupling of the meson current to a nucleon is of order  $N_c^0$  [2]; the additional power of  $N_c$  comes from two nucleon-meson vertices (each of which contributes  $N_c^{1/2}$ ). Thus, these diagrams are consistent with the previously deduced large  $N_c$  scaling behavior

of the potential. However, if one considers a generic crossed-box diagram as shown in Fig. 6, one encounters an inconsistency. Since, the nucleon-meson coupling is generically of order  $\sqrt{N_c}$ , the diagram in Fig. 6 is of order  $N_c^2$ . This scaling, however, violates the proposed large  $N_c$  scaling of the nucleon-nucleon potential (which is supposed to go as  $N_c$ ). Clearly, three and more meson exchange diagrams will yield ever-larger inconsistencies.

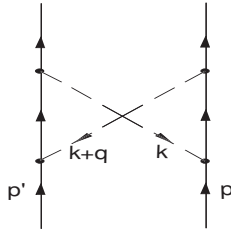


FIG. 6. A crossed-box diagram;  $p = (|\vec{p}|^2/2m_N, -\vec{p})$ ,  $p' = (|\vec{p}'|^2/2m_N, \vec{p}')$ ,  $k = (k^0, \vec{k})$  and  $q = (q^0, \vec{q})$  are energy-momentum 4-vectors.

This paper will also address another central issue in nucleon-nucleon physics; namely, the role of the  $\Delta$  resonance in intermediate states. As is well known, the  $\Delta$  resonance has a low excitation energy for large  $N_c$  (with  $m_\Delta - m_N \sim N_c^{-1}$ ) [4,10]. Moreover, the inclusion of virtual  $\Delta$ 's is known to be essential to ensure the consistency of large  $N_c$  predictions for hadronic processes and its inclusion is necessary for the contracted  $SU(4)$  spin-flavor structure of baryons to be manifest. Thus, one might expect that virtual  $\Delta$ 's will also play a key role in nucleon-nucleon reactions in the large  $N_c$  limit.

In this paper we will show the following picture is consistent with large  $N_c$  QCD:

- i) The nucleon-nucleon interaction can be described by a potential of order  $N_c$  but *not* by a Bethe-Salpeter kernel of order  $N_c$ .
- ii) The meson-exchange picture can be used consistently to describe nucleon-nucleon interactions for momenta of order  $N_c^0$ .
- iii) The meson-exchange picture of the nucleon-nucleon potential (of order  $N_c$ ) breaks down for momenta of order  $N_c$ .
- iv) The leading order nucleon-nucleon potential is symmetric under contracted  $SU(4)$  with corrections down by two powers in  $N_c$  yielding the spin-flavor structure of Ref. [6,7].
- v) The contracted  $SU(4)$  structure implies a central role for intermediate states containing  $\Delta$ 's.

The basic strategy of this paper is to assume that the picture outlined above is correct and then to show that it does not lead to any inconsistencies up to and including two-meson exchange potentials. The key difficulty which must be addressed is the problem of the crossed-box graphs mentioned above: If point ii) is correct then they must be included; however, they generically contribute to the potential at order  $N_c^2$  which exceeds the potential's supposed order  $N_c$  scale from point i). More generally they lead to contributions that are inconsistent with the spin-flavor structure of Refs. [6,7]. However, as we will show, all contributions from the crossed-box graphs which are inconsistent with the spin-flavor structure of Refs. [6,7] are canceled by contributions coming from the retardation effects in the box graphs. While it has long been known that such a cancelation occurs for scalar isoscalar mesons between retardation effects in the box graph and the crossed-box graph [11], it has not been previously shown that such cancelations are far more general and protect the large  $N_c$  structure of the nucleon-nucleon potential including the hierarchy of large and small contributions in terms of spin and isospin. It will also be shown that such a cancelation does not occur if  $\Delta$  intermediate states are excluded or if the momenta of the nucleons is of order  $N_c$ .

## II. REVIEW OF THE $SU(4)$ CONTRACTED SYMMETRY

The baryon sector of large  $N_c$  QCD exhibits an approximate  $SU(4)$  contracted light quark spin-flavor symmetry [3-5]. The contracted  $SU(4)$  algebra is:

$$\begin{aligned} [J^i, J^j] &= i \epsilon_{ijk} J^k, & [I^a, I^b] &= i \epsilon_{abc} I^c, & [J^i, I^a] &= 0, \\ [J^i, X_0^{jb}] &= i \epsilon_{ijk} X_0^{kb}, & [I^a, X_0^{jb}] &= i \epsilon_{abc} X_0^{jc}, & [X_0^{ia}, X_0^{jb}] &= 0, \end{aligned} \quad (1)$$

where  $i, a = 1, 2, 3$  are spin and isospin indices.

TABLE I. Nonrelativistic scalar and pseudo-scalar meson-baryon couplings. The ground state baryons, B, belong to an irreducible representation  $I = J$ .

	Scalars		Pseudo-scalars	
	$I = 0$	$I = 1$	$I = 0$	$I = 1$
meson	$f_0$	$a_0$	$\eta$	$\pi$
meson-baryon coupling	$B^\dagger B \phi$	$B^\dagger I^a B \phi^a$	$B^\dagger J^i B \partial^i \phi$	$B^\dagger X^{ia} B \partial^i \phi^a$
scaling of the coupling	$\sqrt{N_c}$	$(\sqrt{N_c})^{-1}$	$(\sqrt{N_c})^{-1}$	$\sqrt{N_c}$
spin-flavor term	$V_0^0$	$V_0^1$	$V_T^0$	$V_T^1$
KSM scaling	$N_c$	$N_c^{-1}$	$N_c^{-1}$	$N_c$

TABLE II. Nonrelativistic vectors and pseudo-vector meson-baryon couplings. The ground state baryons, B, belong to an irreducible representation  $I = J$ .

	Vectors				Pseudo-vectors	
	$I = 0$		$I = 1$		$I = 0$	$I = 1$
meson	$\omega^t$	$\vec{\omega}$	$\rho^t$	$\vec{\rho}$	$\vec{f}_1$	$\vec{a}_1$
meson-baryon coupling	$B^\dagger B V^t$	$B^\dagger \epsilon_{ijk} J^k B \partial^i V^j$	$B^\dagger I^a B V^{ta}$	$B^\dagger \epsilon_{ijk} X^{ka} B \partial^i V^{ja}$	$B^\dagger J^i B A^i$	$B^\dagger X^{ia} B A^{ia}$
scaling	$\sqrt{N_c}$	$(\sqrt{N_c})^{-1}$	$(\sqrt{N_c})^{-1}$	$\sqrt{N_c}$	$(\sqrt{N_c})^{-1}$	$\sqrt{N_c}$
spin-flavor term	$V_0^0$	$V_T^0$	$V_0^1$	$V_T^1$	$V_\sigma^0$	$V_\sigma^1$
KSM scaling	$N_c$	$N_c^{-1}$	$N_c^{-1}$	$N_c$	$N_c^{-1}$	$N_c$

In large  $N_c$  two-flavor QCD, baryons belong to the infinite dimensional irreducible representation of the contracted  $SU(4)$  algebra with  $I = J = 1/2, 3/2, 5/2, \dots$  [3–5]. For  $N_c = 3$  the  $I = J = 1/2$  and  $I = J = 3/2$  states are identified with nucleon and  $\Delta$ . Other states are presumably a large  $N_c$  artifact. The meson-baryon couplings connecting the states with different spin and isospin are given in terms of the matrix elements of  $X^{ia}$  which is equal to  $X_0^{ia}$  at leading order in the  $1/N_c$  expansion. As shown in Ref. [4], the next-to-leading order term is proportional to  $X_0^{ia}$

$$X^{ia} = \left(1 + \frac{\alpha}{N_c}\right) X_0^{ia} + \mathcal{O}(1/N_c^2), \quad (2)$$

where  $\alpha$  is a constant independent of the spin and isospin indices. As a result, the spin-flavor operators  $X^{ia}$  commute up to  $\mathcal{O}(N_c^{-2})$  corrections:

$$[X^{ia}, X^{jb}] = \mathcal{O}\left(\frac{1}{N_c^2}\right). \quad (3)$$

Meson-baryon couplings satisfying the contracted spin-flavor symmetry are listed in the third row of Table I and Table II. These couplings are obtained from the nonrelativistic reduction of the corresponding covariant Yukawa couplings with corrections suppressed by  $1/N_c$ . The matrix elements of the  $X_0^{ia}$  generators between the baryon states are given in terms of the Clebsch-Gordan coefficients by [4]:

$$\langle I' I_3', J' J_3' | X_0^{ia} | I I_3, J J_3 \rangle = \sqrt{\frac{(2J+1)}{(2J'+1)}} \langle J', J_3' | J J_3; 1 i \rangle \langle I', I_3' | I I_3; 1 a \rangle, \quad (4)$$

where only spin and isospin labels of the baryon states are shown explicitly. A number of useful relations follow from the group algebra (Eq. (1)) [4]:

$$X_0^i X_0^{ib} = \delta^{ab}, \quad X_0^{ia} X_0^{ja} = \delta^{ij}, \quad \epsilon_{ijk} X_0^{ia} X_0^{jb} = \epsilon_{abc} X_0^{kc}. \quad (5)$$

We will need to know the matrix elements of the anticommutators between the nucleon states. When restricting attention to nucleon initial and final states one can easily deduce:

$$\{J^i, X^{ja}\}_{N'N} = \frac{1}{2} \delta^{ij} I^a + \mathcal{O}\left(\frac{1}{N_c^2}\right), \quad \{I^a, X^{ib}\}_{N'N} = \frac{1}{2} \delta^{ab} J^i + \mathcal{O}\left(\frac{1}{N_c^2}\right), \quad (6)$$

where we have used the fact that  $J^i$  and  $I^a$  only take nucleons into nucleons.

The large  $N_c$  scaling of the baryon matrix elements have been analyzed in Refs. [4,5]. Since a general one-quark operator (*e.g.* axial vector current) can couple to any of the  $N_c$  quarks in a baryon, its matrix elements between ground

state baryons are of order  $N_c$  (providing the cancelation between different quark line insertions do not occur). The operators with spin-flavor structure given by  $\mathbf{1}$  and  $X^{ia}$  behave in this leading fashion [4]. On the other hand, currents containing only  $J^i$  and  $I^a$  are of order  $N_c^0$ . Heuristically, the reason is that for baryons with  $J = I = 1/2, 3/2, \dots$  only one out of  $N_c$  quarks carry the spin and isospin quantum numbers of the state. The large  $N_c$  scaling of a meson-baryon coupling is obtained by dividing the corresponding current matrix element by the meson decay constant which is of order  $N_c^{-1/2}$ . Hence, the meson-baryon couplings containing spin-flavor operators  $\mathbf{1}$  or  $X^{ia}$  are of order  $N_c^{1/2}$ . Examples of such leading couplings are the couplings of  $f_0$  and  $\pi$  mesons to baryons. In addition, the time component of  $\omega$  ( $\omega^t$ ) and spatial components of  $\rho$  ( $\vec{\rho}$ ) and  $a_1$  ( $\vec{a}_1$ ) couple to the baryons with a strength proportional  $N_c^{1/2}$ . Couplings containing  $J^i$  and  $I^a$  are of order  $N_c^{-1/2}$ . The examples include the couplings of  $a_0$  and  $\eta$ , spatial components of  $\omega$  and  $f_1$  ( $\vec{\omega}$  and  $\vec{f}_1$ ) and the time component of  $\rho$  ( $\rho^t$ ). These counting rules are listed in the fourth row of Table I and Table II.

Similarly, the spin-flavor structure of the nonrelativistic nucleon-nucleon potential can be analyzed in the large  $N_c$  QCD. The general form of this potential is:

$$V_{NN} = V_0^0 + V_\sigma^0 \vec{\sigma}_{(1)} \cdot \vec{\sigma}_{(2)} + V_T^0 S_{12} + V_{LS}^0 \vec{L} \cdot \vec{S} + V_Q^0 Q_{12} \\ + \left( V_0^1 + V_\sigma^1 \vec{\sigma}_{(1)} \cdot \vec{\sigma}_{(2)} + V_T^1 S_{12} + V_{LS}^1 \vec{L} \cdot \vec{S} + V_Q^1 Q_{12} \right) \vec{\tau}_{(1)} \cdot \vec{\tau}_{(1)}, \quad (7)$$

where

$$S_{12} = 3 \vec{\sigma}_{(1)} \cdot \hat{r} \vec{\sigma}_{(2)} \cdot \hat{r} - \vec{\sigma}_{(1)} \cdot \vec{\sigma}_{(2)}, \quad Q_{12} = \frac{1}{2} \left\{ \vec{\sigma}_{(1)} \cdot \vec{L}, \vec{\sigma}_{(2)} \cdot \vec{L} \right\}, \quad (8)$$

where  $\vec{L}$  and  $\vec{S}$  are the total orbital and spin angular momenta of the system of two nucleons. The operators in Eq. (7) multiplying the position and velocity dependent functions  $V_n^{1,2}$  ( $n = 0, \sigma, T, LS, Q$ ) are referred to as the central, spin-spin, tensor, spin-orbit and quadratic spin-orbit components of the nucleon-nucleon potential in the isosinglet and isotriplet channels.

In Refs. [6,7], the large  $N_c$  scaling of functions  $V_n^{1,2}$  was analyzed using the spin-flavor counting rules of the generators of the contracted  $SU(4)$ . The analysis is based on two assumptions. One is that the nucleon-nucleon interaction can be described by an Hartree Hamiltonian which can be written as a sum of operators with particular spin-flavor structure satisfying the large  $N_c$  scaling rules of the contracted  $SU(4)$  symmetry. In addition, the authors implicitly assumed that the Hartree picture leads to a potential of order  $N_c$  for momenta of order one. At the hadronic level, the latter assumption is essentially equivalent to a one-meson exchange picture of the potential. Based on the above assumptions, the following counting rules were obtained in Refs. [6,7]:

$$V_0^0 \sim V_\sigma^1 \sim V_T^1 \sim N_c, \quad V_0^1 \sim V_\sigma^0 \sim V_T^0 \sim \frac{1}{N_c}. \quad (9)$$

In addition, the spin-orbit and quadratic spin-orbit suppressed by  $1/m_B \sim 1/N_c$  ( $m_B$  is a baryon mass) are of order  $1/N_c^2$ . Note, that the leading order ( $\mathcal{O}(N_c)$ ) components, Eq. (9), are  $SU(4)$  symmetric. The scaling rules in Eq. (9) will be referred to as KSM counting rules.

It is easy to see how the counting rules in Eq. (9) arise from the large  $N_c$  scaling of the meson-baryon couplings at the one-meson exchange level. At this level, a given term in the potential, Eq. (7), scales as the square of the corresponding coupling constant. Since, for example, the isoscalar central potential at leading order gets contributions from  $f_0$  exchange it is of order  $(\sqrt{N_c})^2 = N_c$ . Similarly, the one-pion exchange contributes to the leading part of the isovector tensor term which, therefore, scales as  $(\sqrt{N_c})^2 = N_c$ . On the other hand, the isoscalar tensor potential,  $V_T^0$ , is of order  $N_c^{-1}$  since its leading contribution is from one- $\eta$  exchange. The leading contributions at the one-meson exchange level are shown in the fifth row of Table I and Table II; the  $N_c$  scaling of these contributions are shown in the last row of Table I and Table II. We will show that the nucleon-nucleon potential is consistent with KSM counting rules, Eq. (9), up to and including two-meson exchange contributions.

### III. TWO-MESON EXCHANGE CONTRIBUTIONS

The Feynmann diagrams contributing at the two-meson exchange level are shown in Figs. 4, 6, and 5—the box, the crossed-box and the triangle graphs. In these diagrams the initial and final nucleons are on-mass shell. This condition is necessary if the diagrams are used to derive the nucleon-nucleon potential. The baryon energy-momentum relation is treated nonrelativistically with the baryon propagators having the following form:

$$\frac{i}{k^0 - |\vec{k}|^2/2m_B + i\epsilon} \left( 1 + \mathcal{O}\left(\frac{1}{N_c}\right) \right), \quad (10)$$

where  $k^0$  and  $\vec{k}$  are the energy and the momentum of an intermediate baryon with mass  $m_B$ . In practice,  $m_B = m_N + \mathcal{O}(1/N_c)$  ( $m_N$  is the nucleon mass) for the ground state baryons with  $I = J = 1/2, 3/2, 5/2$ , etc. Relativistic effects are suppressed by  $1/m_B \sim N_c^{-1}$ . The mesons are treated in a fully relativistic form. The meson-baryon vertices are in general momentum and energy dependent. Note, the time and spatial components of  $\omega$  and  $\rho$  have different couplings at leading nonrelativistic order (Table I and Table II). In addition, the spin-flavor structure of  $\omega^t$  coupling is identical to that of  $f_0$  (or  $\sigma$ ). Similarly,  $\rho^t$  and  $a_0$  couplings have identical spin-flavor structure.

A two-meson exchange diagram may contain a piece which is equal to the one iteration of the potential. These contributions will be included when solving the Schrödinger equation and must be excluded from the nucleon-nucleon potential to avoid double counting. This can be illustrated using the two-scalar exchange diagrams.

The contribution to the nucleon-nucleon potential from a one-scalar exchange, Fig. 3, with point couplings is given by,

$$V_{f_0}(\vec{q}) = \frac{g_{f_0}^2}{(q^0)^2 - |\vec{q}|^2 - m_{f_0}^2} = \frac{-g_{f_0}^2}{|\vec{q}|^2 + m_{f_0}^2} \left( 1 + \mathcal{O}(1/N_c^2) \right) \quad (11)$$

where  $m_{f_0}$  ( $\mathcal{O}(N_c^0)$ ) is the mass of the  $f_0$  meson, and the coupling constant  $g_{f_0}$  is of order  $\sqrt{N_c}$  (Table I). Note that  $(q^0)^2$  can be neglected since  $q^0$  is of order  $N_c^{-1}$ .

Similarly, the contribution of the two-scalar exchange box diagram, Fig. 4 to the scattering amplitude,  $\mathcal{M}$ , is

$$i \mathcal{M}_\square = \int \frac{d^3k}{(2\pi)^3} \int \frac{dk^0}{2\pi} \frac{g_{f_0}^4}{((k^0)^2 - |\vec{k}|^2 - m_{f_0}^2)((k^0 + q^0)^2 - |\vec{k} + \vec{q}|^2 - m_{f_0}^2)} \times \frac{1}{(k^0 + |\vec{p}|^2/2m_B - |\vec{p} - \vec{k}|^2/2m_B)(-k^0 + |\vec{p}|^2/2m_B - |\vec{p} - \vec{k}|^2/2m_B)}. \quad (12)$$

It is convenient to first perform the  $k^0$  integral. There are two classes of poles in the complex  $k^0$  plane, namely from the baryon and meson propagators. It is easy to see that the baryon poles in Eq. (12) are on the opposite side of the real  $k^0$  axis. By closing the integration contour in the upper or lower complex plane only one of these baryon poles will contribute to  $\mathcal{M}_\square$ . Closing the contour in the upper plane we get for the baryon pole contribution:

$$i \mathcal{M}_\square^B = \int \frac{d^3k}{(2\pi)^3} \frac{i g_{f_0}^4}{(|\vec{k}|^2 + m_{f_0}^2)(|\vec{k} + \vec{q}|^2 + m_{f_0}^2)(|\vec{p}|^2/m_B - |\vec{p} - \vec{k}|^2/m_B)} \left( 1 + \mathcal{O}\left(\frac{1}{N_c}\right) \right), \quad (13)$$

where, in addition to  $q^0 \sim N_c^{-1}$ , the position of the baryon pole,  $k_B^0 = (|\vec{p}|^2 - |\vec{p} - \vec{k}|^2)/2m_B$ , is neglected when the meson propagators are evaluated. However, the position of the baryon pole is of leading order when the other baryon propagator is evaluated. As will become clear, this value of a baryon propagator is identical to the nonrelativistic Green function in the Lippman-Schwinger equation for the scattering amplitude.

The baryon pole contribution,  $\mathcal{M}_\square^B$ , should be compared with one iterate of the Lippman-Schwinger equation (in the center-of-mass frame):

$$T(\vec{p}, \vec{p} + \vec{q}) = -V(\vec{q}) + \int \frac{d^3k}{(2\pi)^3} V(-\vec{k}) G_0(\vec{k}) T(\vec{p} - \vec{k}, \vec{p} + \vec{q}), \quad (14)$$

where the nonrelativistic baryon Green function is given by

$$G_0(\vec{k}) \equiv \frac{1}{(|\vec{p} - \vec{k}|^2 - |\vec{p}|^2)/m_B + i\epsilon}. \quad (15)$$

The first term in Eq. (14) corresponds to a potential at the one-meson exchange level. For the one-scalar exchange this potential is given in Eq. (11). Iterations of the Lippman-Schwinger equation lead to:

$$T(\vec{p}, \vec{p} + \vec{q}) = -V(\vec{q}) + \int \frac{d^3k}{(2\pi)^3} V(-\vec{k}) G_0(\vec{k}) V(\vec{k} + \vec{q}) - \int \frac{d^3k}{(2\pi)^3} \int \frac{d^3k'}{(2\pi)^3} V(-\vec{k}) G_0(\vec{k}) V(\vec{k} + \vec{k}') G_0(\vec{k}') V(\vec{q} - \vec{k}') + \dots, \quad (16)$$

where the ellipsis indicates higher-order iterations. For the two-scalar exchange, the first iteration of the potential in Eq. (11) is:

$$\int \frac{d^3k}{(2\pi)^3} V_{f_0}(-\vec{k}) G_0(\vec{k}) V_{f_0}(\vec{k} + \vec{q}) = \int \frac{d^3k}{(2\pi)^3} \frac{g_{f_0}^4}{(|\vec{k}|^2 + m_{f_0}^2)(|\vec{k} + \vec{q}|^2 + m_{f_0}^2)(|\vec{p} - \vec{k}|^2/m_B - |\vec{p}|^2/m_B)}, \quad (17)$$

which is exactly equal to the baryon pole contribution,  $\mathcal{M}_\square^B$  (Eq. (13)), evaluated with the nonrelativistic baryon propagator, Eq. (10). Thus, the baryon pole contribution of the two-scalar box diagram should not be included in the nucleon-nucleon potential. Note, that the equality holds only if nonrelativistic baryon propagator is used to evaluate  $\mathcal{M}_\square^B$ .

The remaining contribution to  $\mathcal{M}_\square$  is from the meson poles. This contribution is often referred to as the retardation effect since it is absent when using a static potential. The retardation effect for two-scalar exchange is of order  $N_c^2$  (see Table I), *i.e.* it is larger than allowed by KSM counting rules, Eq. (9). Hence, for the two-scalar exchange diagrams to be consistent with the counting rules, the retardation effect has to be cancelled by the crossed-box diagram. The key issue is whether this cancelation indeed happens.

The baryon pole contribution in the box diagram have been discussed for the two-scalar exchange with point couplings. In fact, it can easily be generalized for any two-meson exchange with general vertex functions. Indeed, the above proof that the baryon pole contribution to the box diagram is one iterate of the potential rests only on the nonrelativistic form of the two-baryon propagators and the direction of the loop momenta and energy flow through the baryon lines. Neither the spin-flavor structure nor the the vertex functions can change the position of the baryon poles. Thus, the baryon poles from any two-meson box diagrams do not contribute to the nucleon-nucleon potential.

We have shown so far that the baryon pole contributions from the two-meson box diagrams should not be included in the nucleon-nucleon potential. However, the retardation effect and the crossed-box can each be larger than allowed by the KSM counting rules. For example, the retardation effect and crossed-box diagrams corresponding to the two-pion exchange are each of order  $N_c^2$ . Moreover, the two-meson exchange diagrams in general can contribute to different spin-flavor structures in the the nucleon-nucleon potential, Eq. (7). As a result, these contributions considered separately may violate the KSM counting rules of the subleading ( $\mathcal{O}(N_c^{-1})$ ) terms in the potential. For example, two-pion exchange box and crossed-box diagrams (each of order  $N_c^2$ ) contribute not only to  $V_T^1$  but among others to isosinglet tensor force,  $V_T^0$ , as well. The latter, however, should be of order  $N_c^{-1}$  according to Eq. (9). Fortunately, as will be shown below, the retardation effects cancel against the crossed-box diagram contributions in all such cases.

A cancelation between the retardation effect and the crossed-box is well known for the two-scalar exchange diagrams [11]. The meson pole contribution to  $\mathcal{M}_\square$ , Eq. (12), is:

$$\begin{aligned} \mathcal{M}_\square^{ret} &= \int \frac{d^3k}{(2\pi)^3} \int \frac{dk^0}{2\pi} 2 \text{Im} \left[ \frac{g_{f_0}^4}{((k^0)^2 - |\vec{k}|^2 - m_{f_0}^2)((k^0 + q^0)^2 - |\vec{k} + \vec{q}|^2 - m_{f_0}^2)} \right] \\ &\quad \times P \left[ \frac{1}{(k^0 + |\vec{p}|^2/2m_B - |\vec{p} - \vec{k}|^2/2m_B)(-k^0 + |\vec{p}|^2/2m_B - |\vec{p} - \vec{k}|^2/2m_B)} \right] \\ &= \int \frac{d^3k}{(2\pi)^3} \frac{g_{f_0}^4}{|\vec{k} + \vec{q}|^2 - |\vec{k}|^2} \left( \frac{1}{2(|\vec{k}|^2 + m_{f_0}^2)^{3/2}} - \frac{1}{2(|\vec{k} + \vec{q}|^2 + m_{f_0}^2)^{3/2}} \right) \left( 1 + \mathcal{O}\left(\frac{1}{N_c}\right) \right), \end{aligned} \quad (18)$$

where in the second step we have again neglected terms in the denominators suppressed by  $1/m_B \sim 1/N_c$  including the energy  $q^0$ ; a symbol  $P$  indicates a principle value.

The contribution to the scattering amplitude from the two-meson crossed-box diagram, Fig. 6, is

$$\begin{aligned} i \mathcal{M}_X &= \int \frac{d^3k}{(2\pi)^3} \int \frac{dk^0}{2\pi} \frac{g_{f_0}^4}{((k^0)^2 - |\vec{k}|^2 - m_{f_0}^2)((k^0 + q^0)^2 - |\vec{k} + \vec{q}|^2 - m_{f_0}^2)} \\ &\quad \times \frac{1}{(k^0 + q^0 + |\vec{p}|^2/2m_B - |\vec{p} + \vec{k} + \vec{q}|^2/2m_B)(k^0 + |\vec{p}|^2/2m_B - |\vec{p} - \vec{k}|^2/2m_B)}. \end{aligned} \quad (19)$$

Note, the baryon poles are now on the same side of the real axis in the  $k^0$  complex plane. Hence, they do not contribute to  $\mathcal{M}_X$ . The only non-vanishing contribution is from the meson poles:

$$\begin{aligned} \mathcal{M}_X &= \int \frac{d^3k}{(2\pi)^3} \int \frac{dk^0}{2\pi} 2 \text{Im} \left[ \frac{g_{f_0}^4}{((k^0)^2 - |\vec{k}|^2 - m_{f_0}^2)((k^0 + q^0)^2 - |\vec{k} + \vec{q}|^2 - m_{f_0}^2)} \right] \\ &\quad \times P \left[ \frac{1}{(k^0 + q^0 + |\vec{p}|^2/2m_B - |\vec{p} + \vec{k} + \vec{q}|^2/2m_B)(k^0 + |\vec{p}|^2/2m_B - |\vec{p} - \vec{k}|^2/2m_B)} \right] \\ &= - \int \frac{d^3k}{(2\pi)^3} \frac{g_{f_0}^4}{|\vec{k} + \vec{q}|^2 - |\vec{k}|^2} \left( \frac{1}{2(|\vec{k}|^2 + m_{f_0}^2)^{3/2}} - \frac{1}{2(|\vec{k} + \vec{q}|^2 + m_{f_0}^2)^{3/2}} \right) \left( 1 + \mathcal{O}\left(\frac{1}{N_c}\right) \right), \end{aligned} \quad (20)$$

where the same approximations as in Eq. (18) were made. As evident from Eqs. (18) and (20), the retardation effect and the the crossed-box diagram contribution for the two-scalar exchange cancel out up to corrections of order  $N_c^{-1}$ :

$$\mathcal{M}_{\square}^{ret} + \mathcal{M}_X = \mathcal{O}\left(\frac{1}{N_c}\right). \quad (21)$$

It is important to stress, however, that the above cancelation does not occur when the nucleon momenta are of order  $N_c$  since for the momenta of order  $N_c$  the baryon propagators evaluated at the meson poles are different (as can be seen from Eqs. (18) and (20)). Consequently, for the momenta of order  $N_c$ , the nucleon-nucleon interaction cannot be interpreted as a simple meson exchange picture consistent with the KSM counting rules, Eq. (9). As will be shown below, the cancelation in Eq. (21) is far more general. In fact, it occurs for all two-meson exchange graphs provided the nucleon momenta are of order  $N_c^0$  and the meson-baryon couplings are contracted  $SU(4)$  symmetric. Let us consider a general box and crossed-box diagram containing any pair of intermediate mesons.

We will use Greek symbols to indicate an exchanged meson, *e.g.*  $\alpha = f_0, \rho, \pi$ , etc. A given graph contains four vertex functions, one for each meson-baryon coupling. The product of these four functions will be denoted by  $\tilde{V}_{\alpha\beta}(k^0, \vec{k}, q^0, \vec{q})$ . The function  $\tilde{V}_{\alpha\beta}(k^0, \vec{k}, q^0, \vec{q})$  does not contain spin-flavor matrices of the corresponding meson-baryon couplings which will be written explicitly. It is clear that  $\tilde{V}_{\alpha\beta} = \tilde{V}_{\beta\alpha}$ . To simplify formulae we combine the product of  $\tilde{V}_{\alpha\beta}(k^0, \vec{k}, q^0, \vec{q})$  and two meson propagators into a single energy-momentum dependent function  $V_{\alpha\beta}(k^0, \vec{k}, q^0, \vec{q})$  defined by

$$V_{\alpha\beta}(k^0, \vec{k}, q^0, \vec{q}) \equiv \frac{\tilde{V}_{\alpha\beta}(k^0, \vec{k}, q^0, \vec{q})}{((k^0)^2 - |\vec{k}|^2 - m_\alpha^2)((k^0 + q^0)^2 - |\vec{k} + \vec{q}|^2 - m_\beta^2)}, \quad (22)$$

where  $m_\alpha$  and  $m_\beta$  are the masses of the  $\alpha$  and  $\beta$  mesons. The above-defined function is symmetric under the interchange of the exchanged mesons,  $V_{\alpha\beta} = V_{\beta\alpha}$ . The analytic structure of  $V_{\alpha\beta}(k^0, \vec{k}, q^0, \vec{q})$  as a function of a complex variable  $k^0$  determines the retardation effects of the box graphs and the contribution of the crossed-box diagrams.

The spin-flavor structure of the meson-baryon vertices will be denoted by  $\Gamma_{\alpha(n)}^A(\vec{k})$  where a superscript  $A$  specifies the spin-flavor indices and subscript  $n = 1, 2$  indicates to which of the two baryon lines a meson couples. The momentum dependence arises in the case of derivatively coupled mesons such as pions. The product of the two  $\Gamma_{\alpha(n)}^A(\vec{k})$  structures at two ends of the same meson propagator are constrained by the spin and isospin of the exchanged meson. To enforce these constraints in the product  $\Gamma_{\alpha(1)}^A(\vec{k})\Gamma_{\alpha(2)}^B(-\vec{k})$ , we introduce a symbol  $C_{AB}^\alpha$ . For example, in the case when the exchanged meson is a pion, the above product takes the form:

$$C_{AB}^\pi \Gamma_{\pi(1)}^A(\vec{k})\Gamma_{\pi(2)}^B(-\vec{k}) = \delta^{ij} \delta^{mn} \delta^{ab} k^j k^n X_{(1)}^{ia} X_{(2)}^{mb} = -k^i k^m X_{(1)}^{ia} X_{(2)}^{ma} \quad (23)$$

where the contracted  $SU(4)$  pion-baryon coupling is used.

Using the above notation a contribution from a general box graph, Fig. 4, has the following form:

$$i \mathcal{M}_{\square} = g_\alpha^2 g_\beta^2 \int \frac{d^3 k}{(2\pi)^3} \int \frac{dk^0}{2\pi} \frac{V_{\alpha\beta}(k^0, \vec{k}, q^0, \vec{q}) C_{AB}^\alpha C_{CD}^\beta \Gamma_{\alpha(1)}^A(\vec{k}) \Gamma_{\beta(1)}^C(-(\vec{k} + \vec{q})) \Gamma_{\alpha(2)}^B(-\vec{k}) \Gamma_{\beta(2)}^D(\vec{k} + \vec{q})}{(k^0 + |\vec{p}|^2/2m_B - |\vec{p} - \vec{k}|^2/2m_B)(-k^0 + |\vec{p}|^2/2m_B - |\vec{p} - \vec{k}|^2/2m_B)}, \quad (24)$$

where  $g_\alpha$  and  $g_\beta$  are the corresponding coupling constants and the momenta directions are shown in Fig. 4. The crossed-box, Fig. 6, has a similar expression with the last two  $\Gamma$ 's interchanged:

$$i \mathcal{M}_X = g_\alpha^2 g_\beta^2 \int \frac{d^3 k}{(2\pi)^3} \int \frac{dk^0}{2\pi} \frac{V_{\alpha\beta}(k^0, \vec{k}, q^0, \vec{q}) C_{AB}^\alpha C_{CD}^\beta \Gamma_{\alpha(1)}^A(\vec{k}) \Gamma_{\beta(1)}^C(-(\vec{k} + \vec{q})) \Gamma_{\beta(2)}^D(\vec{k} + \vec{q}) \Gamma_{\alpha(2)}^B(-\vec{k})}{(k^0 + q^0 + |\vec{p}|^2/2m_B - |\vec{p} + \vec{k} + \vec{q}|^2/2m_B)(k^0 + |\vec{p}|^2/2m_B - |\vec{p} - \vec{k}|^2/2m_B)}. \quad (25)$$

Note the difference in the baryon propagators relative to Eq. (24) due to the difference in the momentum flow.

As was previously shown, the baryon pole contribution to the box-graph is the first iterate of the Lippman-Schwinger equation while these poles do not contribute to the crossed-box graph at this order. As in the case of the scalar exchange, the  $k^0$  integration in Eqs. (24) and (25) can be performed via the contour integration. Whatever the explicit form of the function  $V_{\alpha\beta}(k^0, \vec{k}, q^0, \vec{q})$  its contribution to the  $k^0$  integral is given by its imaginary part. The important point is that the same function appears in  $\mathcal{M}_{\square}$  and  $\mathcal{M}_X$ . Since the intermediate baryons can not go on shell at the meson singularities their contribution equals to the principal values of their propagators.

The retardation effect of the box diagram is:

$$\begin{aligned} \mathcal{M}_{\square}^{ret} &= g_\alpha^2 g_\beta^2 \int \frac{d^3 k}{(2\pi)^3} \int \frac{dk^0}{2\pi} 2 \text{Im} \left[ V_{\alpha\beta}(k^0, \vec{k}, q^0, \vec{q}) \right] C_{AB}^\alpha C_{CD}^\beta \Gamma_{\alpha(1)}^A(\vec{k}) \Gamma_{\beta(1)}^C(-\vec{k} - \vec{q}) \Gamma_{\alpha(2)}^B(-\vec{k}) \Gamma_{\beta(2)}^D(\vec{k} + \vec{q}) \\ &\quad \times P \left[ \frac{1}{(k^0 + |\vec{p}|^2/2m_B - |\vec{p} - \vec{k}|^2/2m_B)} \frac{1}{(-k^0 + |\vec{p}|^2/2m_B - |\vec{p} - \vec{k}|^2/2m_B)} \right] \\ &= g_\alpha^2 g_\beta^2 \int \frac{d^3 k}{(2\pi)^3} \int \frac{dk^0}{2\pi} 2 \text{Im} \left[ V_{\alpha\beta}(k^0, \vec{k}, q^0, \vec{q}) \right] P \left[ -\frac{1}{(k^0)^2} \right] \\ &\quad \times C_{AB}^\alpha C_{CD}^\beta \Gamma_{\alpha(1)}^A(\vec{k}) \Gamma_{\beta(1)}^C(-(\vec{k} + \vec{q})) \Gamma_{\alpha(2)}^B(-\vec{k}) \Gamma_{\beta(2)}^D(\vec{k} + \vec{q}) \left( 1 + \mathcal{O}\left(\frac{1}{N_c}\right) \right). \end{aligned} \quad (26)$$

Similarly, the crossed-box contribution coming entirely from the meson singularities is:

$$\begin{aligned}
\mathcal{M}_X &= g_\alpha^2 g_\beta^2 \int \frac{d^3 k}{(2\pi)^3} \int \frac{dk^0}{2\pi} 2 \operatorname{Im} \left[ V_{\alpha\beta}(k^0, \vec{k}, q^0, \vec{q}) \right] C_{AB}^\alpha C_{CD}^\beta \Gamma_{\alpha(1)}^A(\vec{k}) \Gamma_{\beta(1)}^C(-(\vec{k} + \vec{q})) \Gamma_{\beta(2)}^D(\vec{k} + \vec{q}) \Gamma_{\alpha(2)}^B(-\vec{k}) \\
&\quad \times P \left[ \frac{1}{(k^0 + q^0 + |\vec{p}|^2/2m_B - |\vec{p} + \vec{k} + \vec{q}|^2/2m_B)(k^0 + |\vec{p}|^2/2m_B - |\vec{p} - \vec{k}|^2/2m_B)} \right] \\
&= g_\alpha^2 g_\beta^2 \int \frac{d^3 k}{(2\pi)^3} \int \frac{dk^0}{2\pi} 2 \operatorname{Im} \left[ V_{\alpha\beta}(k^0, \vec{k}, q^0, \vec{q}) \right] P \left[ \frac{1}{(k^0)^2} \right] \\
&\quad \times C_{AB}^\alpha C_{CD}^\beta \Gamma_{\alpha(1)}^A(\vec{k}) \Gamma_{\beta(1)}^C(-(\vec{k} + \vec{q})) \Gamma_{\beta(2)}^D(\vec{k} + \vec{q}) \Gamma_{\alpha(2)}^B(-\vec{k}) \left( 1 + \mathcal{O}\left(\frac{1}{N_c}\right) \right)
\end{aligned} \tag{27}$$

Note that only in the nonrelativistic limit the principal values of the baryon propagators are equal and opposite for both  $\mathcal{M}_\square^{ret}$  and  $\mathcal{M}_X$ . As a result, the sum of these two contributions is proportional to a spin-flavor commutator:

$$\begin{aligned}
\mathcal{M}_\square^{ret} + \mathcal{M}_X &= g_\alpha^2 g_\beta^2 \int \frac{d^3 k}{(2\pi)^3} \int \frac{dk^0}{2\pi} 2 \operatorname{Im} \left[ V_{\alpha\beta}(k^0, \vec{k}, q^0, \vec{q}) \right] P \left[ -\frac{1}{(k^0)^2} \right] \\
&\quad \times C_{AB}^\alpha C_{CD}^\beta \Gamma_{\alpha(1)}^A(\vec{k}) \Gamma_{\beta(1)}^C(-\vec{k} - \vec{q}) \left[ \Gamma_{\alpha(2)}^B(-\vec{k}), \Gamma_{\beta(2)}^D(\vec{k} + \vec{q}) \right] \left( 1 + \mathcal{O}\left(\frac{1}{N_c}\right) \right).
\end{aligned} \tag{28}$$

In general, we have to include both orderings of the exchanged mesons. In Eq. (28) the first meson is  $\alpha$ . Changing the meson sequence and keeping the loop momenta flow unchanged we get,

$$\begin{aligned}
\mathcal{M}_\square^{ret} + \mathcal{M}_X &= g_\alpha^2 g_\beta^2 \int \frac{d^3 k}{(2\pi)^3} \int \frac{dk^0}{2\pi} 2 \operatorname{Im} \left[ V_{\alpha\beta}(k^0, \vec{k}, q^0, \vec{q}) \right] P \left[ -\frac{1}{(k^0)^2} \right] \\
&\quad \times C_{AB}^\alpha C_{CD}^\beta \left[ \Gamma_{\beta(1)}^C(\vec{k}), \Gamma_{\alpha(1)}^A(-\vec{k} - \vec{q}) \right] \Gamma_{\beta(2)}^D(-\vec{k}), \Gamma_{\alpha(2)}^B(\vec{k} + \vec{q}) \left( 1 + \mathcal{O}\left(\frac{1}{N_c}\right) \right),
\end{aligned} \tag{29}$$

where we used  $V_{\beta\alpha} = V_{\alpha\beta}$ . Now, the commutator involves the meson couplings along a different baryon line.

The large  $N_c$  scaling of the retardation effect and the crossed-box diagram taken separately is given by the product of the coupling constants,  $g_\alpha^2 g_\beta^2$ . However, as seen from Eqs. (28) and (29), their total contribution is proportional to the commutators of the spin-flavor operators evaluated between the ground state baryons. The cancelation between the retardation effect and the crossed-box contribution up to higher order corrections happens due to the presence of the commutator.

A number of mesons shown in Table I and Table II make identical contributions to the spin-flavor structure of the nucleon-nucleon potential, Eq. (7). For example, the  $f_0$  and the time component of the  $\omega$  contribute to the isoscalar central potential,  $V_0^0$ ; the  $\pi$  and spatial components of  $\rho$  contribute to isovector tensor force. Other such pairs are  $a_0$  and  $\rho^t$ ,  $\eta$  and  $\vec{\omega}$ ,  $\pi$  and  $\vec{\rho}$ . Thus, out of ten couplings in Table I and Table II there are only six independent structures. They give thirty-six different combinations for two-meson exchange graphs counting combinations differing in the meson sequence. Out of this the number of distinct meson pairs is twenty-one.

The commutators in Eqs. (28) and (29) vanish identically for those graphs in which at least one of the mesons is  $f_0$  (or  $\omega^t$ ). The reason is that the spin-flavor structure of  $f_0$  ( $\omega^t$ ) is given by the unity operator which commutes with any other operator. This insures the large  $N_c$  consistency of the two-meson box and crossed-box diagrams containing the following six (independent) pairs of mesons:

$$(f_0 f_0), (f_0 \vec{f}_1), (f_0 \eta), (f_0 a_0), (f_0 \vec{a}_1), (f_0 \pi), \tag{30}$$

Note, as discussed above the same cancelation occurs when  $\omega^t$  is exchanged instead of  $f_0$ .

Similar cancelations occur for contributions of the box and crossed-box diagrams containing the following pairs of mesons:

$$(a_0 \eta), (a_0 \vec{f}_1), \tag{31}$$

since the spin-flavor structure of  $a_0$  couplings contains only  $I^a$  generators while the couplings of  $\vec{f}_1$  and  $\eta$  contain only  $J^i$  generators which commute with  $I^a$ , Eq. (1).

A number of the meson-baryon couplings in Table I and Table II are of order  $N_c^{-1/2}$ . Hence, the exchange of any pair of such mesons is suppressed by at least  $N_c^{-2}$  and, therefore, cannot violate the KSM counting rules. These are the exchanges of the following meson pairs:

$$(a_0 a_0), (\eta \eta), (\vec{f}_1 \vec{f}_1), (\eta \vec{f}_1), \left[ (a_0 \eta), (a_0 \vec{f}_1) \right], \tag{32}$$

where the meson pairs in the square brackets have been previously considered, Eq. (31).

This leaves us with nine nontrivial meson pair exchanges whose contributions via the box and crossed-box diagrams can potentially spoil the KSM counting rules. Out of these, three pairs couple to baryons only via non-derivative couplings:

$$\begin{aligned} (a_0 \vec{a}_1), (\vec{f}_1 \vec{a}_1), &\rightarrow \mathcal{O}(N_c^0), \\ (\vec{a}_1 \vec{a}_1), &\rightarrow \mathcal{O}(N_c^2), \end{aligned} \quad (33)$$

and the remaining six pairs require one or two derivative couplings:

$$\begin{aligned} (a_0 \pi), (\eta \pi), (\eta \vec{a}_1), (\pi \vec{f}_1), &\rightarrow \mathcal{O}(N_c^0), \\ (\pi \pi), (\pi \vec{a}_1), &\rightarrow \mathcal{O}(N_c^2), \end{aligned} \quad (34)$$

In Eqs. (33) and (34) the large  $N_c$  scaling of the product of corresponding coupling constants,  $g_\alpha^2 g_\beta^2$ , in the box and the crossed-box diagrams has also been indicated.

The considerations of the meson pairs in Eq. (33) are simpler than those with derivatively coupled mesons, Eq. (34), and will be considered first. The analysis of the exchanges with derivative couplings requires performing angular integration and is done in the appendix.

The retardation effect, Eq. (26), and, the crossed-box diagram, Eq. (27), involving exchanges of  $a_0$  and  $\vec{a}_1$  contribute to isoscalar and isovector spin-spin,  $V_\sigma^0$  and  $V_\sigma^1$ , terms; the  $(\vec{f}_1, \vec{a}_1)$  exchange contains a  $V_0^1$  term in addition to  $V_\sigma^1$ . The order  $N_c^0$  contributions to  $V_\sigma^0$  and  $V_0^0$  from  $(a_0, \vec{a}_1)$  and  $(\vec{f}_1, \vec{a}_1)$  exchanges violate the KSM rules, Eq. (9). Fortunately, these contributions are cancelled in the sum of the retardation effect and crossed-box diagram, Eqs. (28) and (29):

$$\begin{aligned} &C_{AB}^{\vec{f}_1} C_{CD}^{\vec{a}_1} \Gamma_{\vec{f}_1(1)}^A(\vec{k}) \Gamma_{\vec{a}_1(1)}^C(-(\vec{k} + \vec{q})) \left[ \Gamma_{\vec{f}_1(2)}^B(-\vec{k}), \Gamma_{\vec{a}_1(2)}^D(\vec{k} + \vec{q}) \right] \\ &= J_{(1)}^i X_{(1)}^{ja} \left[ J_{(2)}^i, X_{(2)}^{ja} \right] = \frac{1}{2} \left( \left\{ J_{(1)}^i, X_{(1)}^{ja} \right\} + \left[ J_{(1)}^i, X_{(1)}^{ja} \right] \right) \left[ J_{(2)}^i, X_{(2)}^{ja} \right] \\ &= 2 X_{(1)}^{ka} X_{(2)}^{ka} + \mathcal{O}\left(\frac{1}{N_c^2}\right), \end{aligned} \quad (35)$$

for  $(\vec{f}_1, \vec{a}_1)$  exchange and similarly for  $(a_0, \vec{a}_1)$  exchange. In the last step in Eq. (35) we used the commutation and anti-commutation relations of the generators of the contracted  $SU(4)$  symmetry, Eqs. (1) and (6). Thus, these exchanges, when both box and crossed-box diagrams are included, contribute only to the isovector spin-spin term of the nucleon-nucleon potential up to corrections of order  $N_c^{-2}$ . This is an allowable contribution by KSM counting rules.

The box and crossed-box diagrams corresponding to  $(\vec{a}_1, \vec{a}_1)$  exchange are of order  $N_c^2$ . The corresponding retardation effect and crossed-box diagram separately contribute to  $V_0^0$ ,  $V_\sigma^1$  and  $V_\sigma^0$ . The first two terms are of order  $N_c$  and the third term is of order  $N_c^{-1}$ , Eq. (9). However, the product of the spin-flavor structures in Eqs. (28) and (29) is of order  $N_c^{-4}$ :

$$\begin{aligned} &C_{AB}^{\vec{a}_1} C_{CD}^{\vec{a}_1} \Gamma_{\vec{a}_1(1)}^A(\vec{k}) \Gamma_{\vec{a}_1(1)}^C(-(\vec{k} + \vec{q})) \left[ \Gamma_{\vec{a}_1(2)}^B(-\vec{k}), \Gamma_{\vec{a}_1(2)}^D(\vec{k} + \vec{q}) \right] \\ &= X_{(1)}^{ia} X_{(1)}^{jb} \left[ X_{(2)}^{ia}, X_{(2)}^{jb} \right] = \frac{1}{2} \left( \left\{ X_{(1)}^{ia}, X_{(1)}^{jb} \right\} + \left[ X_{(1)}^{ia}, X_{(1)}^{jb} \right] \right) \left[ X_{(2)}^{ia}, X_{(2)}^{jb} \right] \\ &= \frac{1}{2} \left[ X_{(1)}^{ia}, X_{(1)}^{jb} \right] \left[ X_{(2)}^{ia}, X_{(2)}^{jb} \right] \sim \mathcal{O}\left(\frac{1}{N_c^4}\right), \end{aligned} \quad (36)$$

where in the third step we used the fact that the anticommutator is symmetric and the commutator is antisymmetric under the simultaneous exchange of the spin-flavor indices  $(ia) \rightarrow (jb)$ ; the large  $N_c$  of the baryon matrix elements of  $[X^{ia}, X^{jb}]$  is given in Eq. (2). Combining the  $N_c^4$  suppression in Eq. (36) with the  $N_c^2$  scaling of the product  $g_{\vec{a}_1}^4$  we see that the sum in Eq. (28) (and similarly in Eq. (29)) is of order  $N_c^{-2}$  which is consistent with KSM counting rules. Note that in this case full contracted  $SU(4)$  algebra has to be used to insure the cancellation. Thus, the cancellation of the retardation effect against the crossed-box diagram requires an inclusion of both nucleon and  $\Delta$  intermediate states. If one restricts the intermediate states to nucleons only, the cancellation would not occur.

Thus far, we have shown that the retardation effect of all two-meson exchange diagrams without derivative couplings, Eq. (33), cancel against the corresponding crossed-box graphs. As is shown in the appendix, similar cancellations occur for the remaining six meson pairs, Eq. (34), which involve one or two derivatively coupled mesons.

In addition to box and crossed-box diagrams, any pair of mesons can be exchanged via triangle (or ‘‘seagull’’) diagrams, Fig. 5, containing a 4-point meson-baryon vertex. The spin-flavor structure of this vertex is given by

the product of two  $\Gamma_{\alpha(n)}^A(\vec{k})$  operators. The 4-point meson-baryon coupling is of order  $N_c^0$  for any meson pair [2]. Hence, the largest scaling of a triangle diagram is  $N_c$ , *e.g.* when two pions or  $f_0$  and  $\omega^t$  are exchanged. Thus, the triangle graph can not violate the scaling of the leading ( $\mathcal{O}(N_c)$ ) spin-flavor terms, Eq. (9). However, the subleading ( $\mathcal{O}(N_c^{-1})$ ) terms might be sensitive to contributions from the triangle diagrams. Since these diagrams contain only one baryon propagator its pole does not contribute to the potential (the contour of the complex  $k^0$  integration can always be closed in such a way as to avoid the baryon pole). As we will show shortly, the contributions from the meson singularities in the triangle graphs add up to cancel all terms that violate the KSM counting rules.

A given triangle graph can be associated with a corresponding box or crossed-box diagram by shrinking the appropriate baryon propagator to zero. It can then be shown that the sum of the appropriate pair of the triangle graphs, shown in Fig. 5, is similar to Eq. (28) or Eq. (29). The essential point in the above discussion was the presence of the commutator in Eqs. (28) and (29). The same commutator appears in the sum of the triangle graphs.

What are the pairs of the triangle graphs that correspond to the box and crossed-box diagrams which led to Eqs. (28) and (29)? These graphs contain the same meson pairs. The two corresponding graphs differ according to which baryon line the 4-point meson-baryon vertex is attached, Fig. 5. In addition, two  $\Gamma$  structures at the 4-point vertex of one of the corresponding graphs are in opposite order relative to the sequence of these structures in the other graph. This leads to the appearance of a commutator in the sum of the corresponding triangle graphs.

In the case of the box and crossed-box diagrams the direction of the energy flow assured that the retardation effect and the crossed-box contribution are equal and opposite up to  $1/N_c$  corrections. The sign difference was due to the product of the principle values of the baryon propagators (after the nonrelativistic reduction), Eqs. (26) and (27), which had different signs for the box and crossed-box diagrams. Despite the presence of only a single baryon propagator, the contributions from each of the corresponding triangle graphs come with opposite signs due to the different flow of the energy and momenta, Fig. 5. The sum of these two graphs is:

$$\begin{aligned} \mathcal{M}_1 + \mathcal{M}_2 &= g_\alpha g_\beta g_{\alpha\beta} \int \frac{d^3k}{(2\pi)^3} \int \frac{dk^0}{2\pi} 2 \text{Im} \left[ V_{\alpha\beta}(k^0, \vec{k}, q^0, \vec{q}) \right] P \left[ -\frac{1}{k^0} \right] \\ &\times C_{AB}^\alpha C_{CD}^\beta \Gamma_{\alpha(1)}^A(\vec{k}) \Gamma_{\beta(1)}^C(-\vec{k} - \vec{q}) \left[ \Gamma_{\alpha(2)}^B(-\vec{k}), \Gamma_{\beta(2)}^D(\vec{k} + \vec{q}) \right] \left( 1 + \mathcal{O}\left(\frac{1}{N_c}\right) \right), \end{aligned} \quad (37)$$

where  $g_{\alpha\beta}$  (order  $N_c^0$  for all  $\alpha$  and  $\beta$ ) is the coupling constant of the 4-point vertex and the function  $V_{\alpha\beta}$  is given by Eq. (22) provided  $\tilde{V}_{\alpha\beta}$  contains the product of the three meson baryon vertex functions (including one corresponding to 4-point vertex). A similar expression can be written for the sum of the two triangle graphs in which the sequence of the  $\alpha$  and  $\beta$  mesons is changed as in Eq. (29).

It is clear that the sum in Eq. (37) contributes to the same spin-flavor terms as the sum in Eq. (28): both expressions contain identical spin-flavor structures. The differences in the integrands are irrelevant as far as the cancelations in Eqs. (28) and (29) are concerned. As a result, the large  $N_c$  scaling of the contribution in Eq. (37) is that of Eq. (28) times scaling of  $(g_\alpha g_\beta)^{-1}$ .

Hence, when all the contributions of the triangle graphs are included the resulting spin-flavor terms are consistent with the KSM counting rules, Eq. (9).

#### IV. CONCLUSION

At a technical level we have shown by explicit calculation that if meson-baryon couplings scale according to the standard large  $N_c$  rules, then the two-meson-exchange contributions to the nonrelativistic baryon-baryon potential is consistent with the large  $N_c$  KSM scaling rules deduced in Refs. [6,7]. This is highly nontrivial since the derivation of these rules in Refs. [6,7] only included diagrams which correspond to one-meson-exchange when translated to the hadronic level. This certainly adds confidence that Refs. [6,7] correctly described the  $N_c$  scaling behavior of the nucleon-nucleon potential in the large  $N_c$  limit of QCD. The essential issue in the calculations here was that the retardation contributions to the potential from the box graph cancel against the crossed-box contributions for all spin-isospin structures in the potential where the retardation contributions or the crossed-box contributions separately violate the counting rules.

The derivation presented here was done in a “brute force” manner. Namely, we considered the various meson exchanges one at a time, identified the contributions to the various spin-isospin structures which apparently violated the KSM large  $N_c$  scalings and showed that in all cases they canceled. It would be very useful to find a more general method for demonstrating the cancelation. While the methods used here were adequate for the two-meson exchange case, it would be extremely cumbersome to extend them to three-meson exchange or higher. Given the cancelations for all “dangerous” contributions at the two-meson-exchange level it seems reasonable to expect that such cancelations

will occur for any number of meson exchanges and that the full baryon-baryon potential will be consistent with the KSM scaling rules. However, a general proof of the cancelations for all orders would be desirable.

In the Introduction it was argued that the large  $N_c$  scaling behavior of the baryon-baryon interactions give some general insights into the underlying physics arising from QCD. In particular it was argued that a consistent picture emerged and five aspects of this picture were enumerated. Let us now briefly discuss how the calculations discussed above support this picture.

The first point raised was that while a nonrelativistic potential used to describe the interaction has overall strength of order  $N_c$ , the kernel of a Bethe-Salpeter equation does not have a simple  $N_c$  dependence. As noted many times, the order  $N_c^2$  contribution to the potential from the crossed-box graph is canceled by the retardation effect from the box graph. However, such a cancelation cannot happen in the context of the Bethe-Salpeter equation. The entire box graph (including meson pole contributions) is an iterate of the Bethe-Salpeter kernel and hence cannot be included as a contribution to the kernel. Thus, in the Bethe-Salpeter context there is no part of the box graph to cancel the order  $N_c^2$  contribution from the crossed-box. Therefore, unlike the potential, the Bethe-Salpeter kernel cannot be associated with an overall strength of  $N_c$ . Presumably, the Bethe-Salpeter kernel has contributions scaling as  $N_c$  to all powers arising from multiple meson exchanges.

The second point made was that the meson exchange picture of baryon-baryon interactions with the leading part of the potential scaling as  $N_c$  is consistent with the meson exchange picture of the potential provided the momentum exchanged is of order  $N_c^0$ . It was shown explicitly using nonrelativistic kinematics that at the level of two-meson exchange all “dangerous” contributions to the potential canceled so that there is no inconsistency with a potential scaling as  $N_c$ . It is reasonable to expect the behavior to hold for any number of meson exchanges. If true, this strengthens the case for using meson exchange models to describe nucleon-nucleon interactions.

However, it was also argued that the idea of a potential described by the meson exchange picture is unsuitable for momenta of order  $N_c$ . At a technical level this is apparent in Eqs. (18), (19), (25) and (26) where the cancelations of the box and crossed box graphs depend explicitly on the nonrelativistic form of the propagator. If momenta of order  $N_c$  were used the cancelations clearly fail to occur. Thus the usefulness of the meson-exchange picture is not evident for momenta of order  $N_c$ . In fact, it is quite satisfying that the evidence of consistency breaks down in this regime for a number of reasons. In the first place Witten’s TDH picture of baryon-baryon interactions is more appropriate for  $p \sim N_c$ . This picture has no obvious meson-exchange interpretation. The internal structure of each baryon is distorted in the presence of the other. Moreover, it is not surprising from a more traditional hadronic viewpoint that a meson-exchange potential picture breaks down in this regime. If  $p \sim N_c$  and  $m_N \sim N_c$  then the kinetic energy of the baryons is also of order  $N_c$ . Since meson masses are of order  $N_c^0$  an increasing number of mesons are produced. It is hardly surprising that the potential picture breaks down in this situation.

A fourth point raised in the Introduction was that relative sizes of the various spin-isospin structures in the nucleon-nucleon potential are consistent at the two-meson-exchange level with those deduced from the contracted  $SU(4)$  structure of KSM. Moreover, if one looks carefully at all of the cancelations, one finds that corrections to the leading behavior were all  $1/N_c^2$  suppressed. This is consistent with Refs. [6,7] where it is found that subleading spin-isospin structures are down by factors  $1/N_c^2$ . Overall this strongly supports the view that the expansion is in fact in  $1/N_c^2$  rather than in  $1/N_c$ .

The final point stressed was that the  $\Delta$  plays an essential role. As is evident from Eqs. (36) and the appendix, the cancelations between the box and crossed-box graphs do not occur if intermediate states are restricted entirely to nucleons;  $\Delta$  resonances are required as intermediate states. More generally one expects that as the contracted  $SU(4)$  structure is used to obtain cancelations the entire  $I = J = 1/2, 3/2, 5/2, \dots$  tower of baryon states can contribute. Up to two-meson exchange with nucleon as initial and final states, however, only nucleons and  $\Delta$ ’s can contribute.

The formal consistency of the large  $N_c$  treatment and the meson exchange picture is quite satisfying. However, considerable caution should be exercised in trying to draw conclusions about the real world of  $N_c = 3$ . We have used  $1/N_c$  as a counting parameter to distinguish large from small contributions. This is clearly legitimate if all the coefficients multiplying these factors are natural, *i.e.* of order unity. However, all coefficients are not natural. One key difficulty is that the meson-exchange picture is being used here to connect hadronic phenomena with nuclear phenomena. However, the scales in nuclear physics are generally much smaller than those in hadronic physics [5]. It is not clear directly from QCD why these nuclear scales are so small and it is generally thought to be “accidental”. The interplay between small nuclear scales (that may be large in a  $1/N_c$  sense) with much larger hadronic scales (that may be small formally in a  $1/N_c$  sense) can potentially spoil the results of a straightforward  $1/N_c$  approach. To show how extreme this problem may be we can consider the deuteron binding energy,  $B$  (which is formally of order  $N_c$ ) and the delta-nucleon mass difference,  $m_\Delta - m_N$  (which is order  $1/N_c$ ). If all coefficients were natural, one would expect  $B$  to be an order of magnitude larger than  $m_\Delta - m_N$ , whereas, in fact, it is two orders of magnitude smaller. It would not be surprising that difficulties might arise when calculating  $B$  if one neglects  $m_\Delta - m_N$  as being “small”.

The large  $N_c$  structure of the nucleon-nucleon potential has been so far used phenomenologically in two contexts. The first is as an attempt to justify the observed approximate Wigner  $SU(4)$  symmetry [12] in light nuclei as arising

from the underlying contracted  $SU(4)$  structure in the large  $N_c$  potential [6]. The second is an attempt to justify the qualitative sizes of the spin-flavor structures in phenomenological potentials as being explained by contracted  $SU(4)$  structure in the large  $N_c$  potential [6,7]. It is not immediately obvious that these two explanations are legitimate in light of qualitatively distinct nuclear scales that are not associated with the  $1/N_c$  expansion. Clearly, this issue needs further investigation. However, it is also not immediately clear how to formulate a systematic expansion which both incorporates the  $1/N_c$  scaling rules while allowing nuclear scales to be much smaller than hadronic scales. The comparison of the qualitative sizes of the spin-flavor structures in phenomenological potentials with what is expected from large  $N_c$  raises another issue. The potentials predicted in large  $N_c$  are not nucleon-nucleon potentials; rather, they are coupled channel potentials for the full tower of  $I = J$  baryon states including an explicit  $\Delta$ . The phenomenological potentials to which they are compared have the explicit  $\Delta$ 's integrated out. It is by no means clear that the act of integrating out  $\Delta$ 's does not alter the spin-flavor structure. Again, this requires further study.

Given these possible difficulties in drawing phenomenological conclusions from large  $N_c$  potentials, one might ask about the relevance for the real world of our demonstration that large  $N_c$  counting rules are consistent with the meson-exchange picture of potentials at the two-meson-exchange level. Of course, it remains possible that after a careful study one may find that the particular phenomenological predictions to date—the Wigner  $SU(4)$  symmetry and the characteristic relative sizes of the various terms in phenomenological potentials—are robust and remain valid even after the smallness of the typical nuclear scales are included. Whether or not this turns out to be the case, however, we may still be able to learn qualitatively interesting things. For example, the cancelations seen in the two-pion exchange graphs require that  $\Delta$  intermediate states be included. For  $N_c = 3$ , one does not expect such cancelations to be perfect, but the general tendency to cancel should survive. This suggests that  $\Delta$  box and crossed-box contributions should be comparable in size to the ones with nucleon intermediate states. This issue may be relevant for potential models motivated by chiral symmetry where two-pion exchange contributions with nuclear intermediate states are included at next-to-leading order but explicit  $\Delta$  contributions are not included [5]. At a more qualitative level, the fact that at large  $N_c$  a meson-exchange motivated picture of the potential is consistent gives at least some support for the view that more generally nucleon-nucleon interactions can be described in terms of meson exchanges.

## ACKNOWLEDGMENTS

This work is supported by the U.S. Department of Energy grant DE-FG02-93ER-40762. TDC wishes to acknowledge discussions with M. Luty, D. Phillips, J. Friar, F. Gross and S. Wallace. He also acknowledges support at the INT where progress was made on this work.

## APPENDIX:

In this appendix we discuss the box and crossed-box graphs with one or two derivative couplings, Eq. (34). As in the case of the non-derivatively coupled mesons, Eq. (33), the sum of the retardation effect and the crossed-box diagram can be written as the sum of the products of anticommutators and commutators of the spin-flavor generators. The cancelation of the terms that violated spin-flavor counting rules essentially has occurred due the symmetry properties of this products under the interchange of the spin-flavor symmetry. The remaining terms are either consistent with the counting rules or suppressed by  $1/N_c^2$  as in Eq. (36). However, when derivatively coupled mesons are included the symmetry of the products of commutators and anticommutators under the interchange of spin-flavor symmetry is broken due to the contraction of the spin-flavor generators with momentum indices. In order to see the cancelation the angular integration in Eqs. (28) and (29) must be performed. In this appendix the cancelation is shown for the two-pion exchange diagrams. The exchanges involving other pairs of mesons, Eq. (34), are essentially identical to this case.

The retardation effect and the crossed-box contribution is given in Eq. (28) which has the following form for the two-pion exchange:

$$\begin{aligned} \mathcal{M}_{\square}^{ret} + \mathcal{M}_X &= g_\pi^4 \int \frac{d^3 k}{(2\pi)^3} \int \frac{dk^0}{2\pi} P \left[ -\frac{1}{(k^0)^2} \right] 2 \text{Im} \left[ V_{\pi\pi}(k^0, \vec{k}, q^0, \vec{q}) \right] \\ &\times X_{(1)}^{ia} X_{(1)}^{jb} \left[ X_{(2)}^{la}, X_{(2)}^{rb} \right] \vec{k}^i \vec{k}^j (\vec{k}^l + \vec{q}^l) (\vec{k}^r + \vec{q}^r) \left( 1 + \mathcal{O}\left(\frac{1}{N_c}\right) \right). \end{aligned} \quad (\text{A1})$$

After  $k^0$  integration Eq. (A1) reduces to

$$\mathcal{M}_{\square}^{ret} + \mathcal{M}_X = g_\pi^4 \int \frac{k^2 dk}{(2\pi)^3} \int d\Omega F(|\vec{k}|, |\vec{q}|, \vec{k} \cdot \vec{q}, q^0) X_{(1)}^{ia} X_{(1)}^{jb} \left[ X_{(2)}^{la}, X_{(2)}^{rb} \right] \vec{k}^i \vec{k}^j (\vec{k}^l + \vec{q}^l) (\vec{k}^r + \vec{q}^r), \quad (\text{A2})$$

where the explicit form of the function  $F(|\vec{k}|, |\vec{q}|, \vec{k} \cdot \vec{q}, q^0)$  is not required for the following discussion.

Let us consider the angular integration in Eq. (A2):

$$I_\Omega \equiv \int d\Omega F(|\vec{k}|, |\vec{q}|, \vec{k} \cdot \vec{q}, q^0) \vec{k}^i \vec{k}^j (\vec{k}^l + \vec{q}^l) (\vec{k}^r + \vec{q}^r). \quad (\text{A3})$$

The general form of this integral is:

$$\begin{aligned} I_\Omega = & (\delta^{ij} \delta^{lr} + \delta^{il} \delta^{jr} + \delta^{ir} \delta^{jl}) f_1(|\vec{k}|, |\vec{q}|, q^0) + q^i q^j q^l q^r f_2(|\vec{k}|, |\vec{q}|, q^0) \\ & + (\delta^{ij} q^l q^r + \delta^{lr} q^i q^j) f_3(|\vec{k}|, |\vec{q}|, q^0) \\ & + (\delta^{il} q^j q^r + \delta^{ir} q^j q^l + \delta^{jr} q^i q^l + \delta^{jl} q^i q^r) f_4(|\vec{k}|, |\vec{q}|, q^0), \end{aligned} \quad (\text{A4})$$

where functions  $f_1, f_2, f_3$  and  $f_4$  do not depend on  $\vec{k} \cdot \vec{q}$ . The form of the  $I_\Omega$  can be obtained from general arguments based on the symmetry properties of Eq. (A3) under the various exchanges of the momentum indices.

Each term in Eq. (A4) when combined with spin-flavor generators in Eq. (A1) is suppressed by  $N_c^{-4}$ . Let us see how it comes about for each term separately.

The first product of Kronecker deltas in the  $f_1$  term leads to:

$$\begin{aligned} \delta^{ij} \delta^{lr} X_{(1)}^{ia} X_{(1)}^{jb} [X_{(2)}^{la}, X_{(2)}^{rb}] &= X_{(1)}^{ia} X_{(1)}^{ib} [X_{(2)}^{la}, X_{(2)}^{lb}] \\ &= \frac{1}{2} \left( \{X_{(1)}^{ia}, X_{(1)}^{ib}\} + [X_{(1)}^{ia}, X_{(1)}^{ib}] \right) [X_{(2)}^{la}, X_{(2)}^{lb}] \\ &= \frac{1}{2} \{X_{(1)}^{ia}, X_{(1)}^{ib}\} [X_{(2)}^{la}, X_{(2)}^{lb}] + \frac{1}{2} [X_{(1)}^{ia}, X_{(1)}^{ib}] [X_{(2)}^{la}, X_{(2)}^{lb}] \sim \mathcal{O}\left(\frac{1}{N_c^4}\right), \end{aligned} \quad (\text{A5})$$

where the product of the commutator and the anticommutator vanishes because the commutator is antisymmetric under the  $a \leftrightarrow b$  exchange while the anticommutator is symmetric. The remaining product of the two commutators is of order  $N_c^{-4}$  from Eq. (3). Thus, an overall contribution of this term is of order  $N_c^{-2}$  which is consistent with KSM counting rules, Eq. (9). Note how the angular averaging of Eq. (A3) induced symmetry properties of the spin-flavor matrices in Eq. (A1).

The second product of deltas in  $f_1$  leads to the expression identical to Eq. (36); its contribution, therefore, is suppressed by  $N_c^{-4}$  as well. The suppression of the last term multiplying the  $f_1$  are easily observed:

$$\begin{aligned} \delta^{ir} \delta^{jl} X_{(1)}^{ia} X_{(1)}^{jb} [X_{(2)}^{la}, X_{(2)}^{rb}] &= X_{(1)}^{ia} X_{(1)}^{ib} [X_{(2)}^{ja}, X_{(2)}^{ib}] \\ &= \frac{1}{2} \left( \{X_{(1)}^{ia}, X_{(1)}^{jb}\} + [X_{(1)}^{ia}, X_{(1)}^{jb}] \right) [X_{(2)}^{ja}, X_{(2)}^{ib}] \\ &= \frac{1}{2} \{X_{(1)}^{ia}, X_{(1)}^{jb}\} [X_{(2)}^{ja}, X_{(2)}^{ib}] + \mathcal{O}\left(\frac{1}{N_c^4}\right) = \mathcal{O}\left(\frac{1}{N_c^4}\right), \end{aligned} \quad (\text{A6})$$

where in the last step we used antisymmetry under the simultaneous exchange of  $a \leftrightarrow b$  and  $i \leftrightarrow j$ :

$$\{X_{(1)}^{ia}, X_{(1)}^{jb}\} [X_{(2)}^{ja}, X_{(2)}^{ib}] = - \{X_{(1)}^{ia}, X_{(1)}^{jb}\} [X_{(2)}^{ja}, X_{(2)}^{ib}]. \quad (\text{A7})$$

Similarly the product of the 4 components of the external momenta multiplying  $f_2$  is of order  $N_c^{-4}$ :

$$\begin{aligned} q^i q^j q^l q^r X_{(1)}^{ia} X_{(1)}^{jb} [X_{(2)}^{la}, X_{(2)}^{rb}] \\ = \frac{1}{2} q^i q^j q^l q^r \{X_{(1)}^{ia}, X_{(1)}^{jb}\} [X_{(2)}^{la}, X_{(2)}^{rb}] + \mathcal{O}\left(\frac{1}{N_c^4}\right) = \mathcal{O}\left(\frac{1}{N_c^4}\right), \end{aligned} \quad (\text{A8})$$

where the vanishing of the last product can be seen after the substitution  $a \leftrightarrow b, i \leftrightarrow j$  and  $l \leftrightarrow r$ :

$$q^i q^j q^l q^r \{X_{(1)}^{ia}, X_{(1)}^{jb}\} [X_{(2)}^{la}, X_{(2)}^{rb}] = -q^i q^j q^l q^r \{X_{(1)}^{ia}, X_{(1)}^{jb}\} [X_{(2)}^{la}, X_{(2)}^{rb}]. \quad (\text{A9})$$

To show the suppression of the  $f_3$  term in Eq. (A3) we need to use Eqs. (2), (3) and (5):

$$\begin{aligned} \delta^{ij} q^l q^r X_{(1)}^{ia} X_{(1)}^{jb} [X_{(2)}^{la}, X_{(2)}^{rb}] &= q^l q^r X_{(1)}^{ia} X_{(1)}^{ib} [X_{(2)}^{la}, X_{(2)}^{rb}] \\ &= q^l q^r \delta^{ab} \left(1 + \frac{2\alpha}{N_c}\right) [X_{(2)}^{la}, X_{(2)}^{rb}] + \mathcal{O}\left(\frac{1}{N_c^4}\right) \\ &= q^l q^r \left(1 + \frac{2\alpha}{N_c}\right) [X_{(2)}^{la}, X_{(2)}^{ra}] + \mathcal{O}\left(\frac{1}{N_c^4}\right) = \mathcal{O}\left(\frac{1}{N_c^4}\right), \end{aligned} \quad (\text{A10})$$

where the last product vanishes which can be seen via the substitution  $l \leftrightarrow r$ . Similar arguments apply for the second term in  $f_3$ .

The remaining term in Eq. (A3) multiplying  $f_4$  contains four products. This sum vanishes (up to  $\mathcal{O}(N_c^{-4})$ ) as follows:

$$\begin{aligned}
& (\delta^{il} q^j q^r + \delta^{ir} q^j q^l + \delta^{jr} q^i q^l + \delta^{jl} q^i q^r) X_{(1)}^{ia} X_{(1)}^{jb} \left[ X_{(2)}^{la}, X_{(2)}^{rb} \right] \\
&= q^j q^r X_{(1)}^{ia} X_{(1)}^{jb} \left[ X_{(2)}^{ia}, X_{(2)}^{rb} \right] + q^j q^l X_{(1)}^{ia} X_{(1)}^{jb} \left[ X_{(2)}^{la}, X_{(2)}^{ib} \right] \\
&+ q^i q^l X_{(1)}^{ia} X_{(1)}^{jb} \left[ X_{(2)}^{la}, X_{(2)}^{jb} \right] + q^i q^r X_{(1)}^{ia} X_{(1)}^{jb} \left[ X_{(2)}^{ja}, X_{(2)}^{rb} \right] \\
&= q^j q^l X_{(1)}^{ia} X_{(1)}^{jb} \left[ X_{(2)}^{ia}, X_{(2)}^{lb} \right] + q^j q^l X_{(1)}^{ia} X_{(1)}^{jb} \left[ X_{(2)}^{la}, X_{(2)}^{ib} \right] \\
&+ q^i q^l X_{(1)}^{ia} X_{(1)}^{jb} \left[ X_{(2)}^{la}, X_{(2)}^{jb} \right] + q^i q^l X_{(1)}^{ia} X_{(1)}^{jb} \left[ X_{(2)}^{ja}, X_{(2)}^{lb} \right], \tag{A11}
\end{aligned}$$

where in the first step we changed the dummy index  $r$  into  $l$  in the first and the fourth terms; next, we make the  $j \leftrightarrow l$  exchange in the first two terms and  $i \leftrightarrow l$  exchange in the last two terms; finally, making the interchange  $a \leftrightarrow b$  in the second and the fourth terms and collecting the appropriate terms we get:

$$\begin{aligned}
& q^j q^l \left( X_{(1)}^{ia} X_{(1)}^{lb} - X_{(1)}^{ib} X_{(1)}^{la} \right) \left[ X_{(2)}^{ia}, X_{(2)}^{jb} \right] + q^i q^l \left( X_{(1)}^{la} X_{(1)}^{jb} - X_{(1)}^{lb} X_{(1)}^{ja} \right) \left[ X_{(2)}^{ia}, X_{(2)}^{jb} \right] \\
&= q^j q^l \left( \left[ X_{(1)}^{ia}, X_{(1)}^{lb} \right] - \left[ X_{(1)}^{ib}, X_{(1)}^{la} \right] \right) \left[ X_{(2)}^{ia}, X_{(2)}^{jb} \right] = \mathcal{O}\left(\frac{1}{N_c^4}\right). \tag{A12}
\end{aligned}$$

where in the last step we changed  $i \leftrightarrow j$  and  $a \leftrightarrow b$  in the second term.

This completes the discussion of two-pion exchange box and crossed-box diagrams. Their mutual contribution has an overall scaling of  $N_c^{-2}$  and is, therefore, consistent with the KSM counting rules, Eq. (9).

- [1] G. 't Hooft, Nucl. Phys. **B72** 461 (1974).
- [2] E. Witten, Nucl. Phys. **B160** 57 (1979).
- [3] J.L. Gervais and B. Sakita, Phys. Rev. Lett. **52** 87 (1984);  
J.L. Gervais and B. Sakita, Phys. Rev. **D30** 1795 (1984);  
C. Carone, H. Georgi, S. Osofsky, Phys. Lett. **B322** 227 (1994);  
M. Luty and J. March-Russell, Nucl. Phys. **B426** 71 (1994).
- [4] R. Dashen, E. Jenkins and A.V. Manohar, Phys. Rev. **D49** 4713 (1994).
- [5] R. Dashen, E. Jenkins and A.V. Manohar, Phys. Rev. **D51** 3697 (1995).
- [6] D.B. Kaplan and M.J. Savage, Phys. Lett. **B365** 244 (1996).
- [7] D.B. Kaplan and A.V. Manohar, Phys. Rev. **C56** 76 (1997).
- [8] R. Machleidt, K. Holinde and Ch. Elster, Phys. Rep. **149** 1 (1987).
- [9] M.M. Nagels, T.A. Rijken and J.J. de Swart, Phys. Rev. **D17** 768 (1978);  
R. Wiringa, R. Smith and T. Ainsworth, Phys. Rev. **C29** 1207 (1984).
- [10] G.S. Adkins, C.R. Nappi and E. Witten, Nucl. Phys. **B228** 552 (1983).
- [11] F. Gross, Phys. Rev. **186** 1448 (1969); F. Gross, Phys. Rev. **C26** 2203 (1982);  
F. Gross, Relativistic Quantum Mechanics and Field Theory (Wiley, 1993).
- [12] E. Wigner, Phys. Rev. **51** 106, 947 (1937); *ibid.* **56** 519 (1939).
- [13] S. Weinberg, Phys. Lett. **B251** 288 (1990); S. Weinberg, Nucl. Phys. **B363** 3 (1991);  
C. Ordóñez and U. van Kolck, Phys. Lett. **B291** 459 (1992);  
C. Ordóñez, L. Ray and U. van Kolck, Phys. Rev. Lett. **72** 1982 (1994);  
E. Epelbaum, W. Glöckle and Ulf-G. Meißner, Nucl. Phys. **A637** 107 (1998);  
E. Epelbaum, W. Glöckle and Ulf-G. Meißner, Nucl. Phys. **A671** 295 (2000).